Liquid Crystals, 2013
Vol. 40, No. 5, 605–615, http://dx.doi.org/10.1080/02678292.2013.774064

Taylor & Francis
Taylor & Francis Group

ORIGINAL ARTICLE

Liquid crystals with negative dielectric anisotropy: the effect of unsaturation in the terminal chain on thermal and electro-optical properties

Aleksandra Jankowiak[a], Bryan Ringstrand[a,b], Adam Januszko[a,c], Piotr Kaszynski[a,d]* and Michael D. Wand[e]

[a]*Organic Materials Research Group, Department of Chemistry, Vanderbilt University, Nashville, TN 37235, USA;* [b]*Current address: Materials Science Division, Argonne National Laboratory, Argonne, IL 60439, USA;* [c]*Current address: Department of New Technology and Chemistry, Military University of Technology, Warsaw, Poland;* [d]*Section of Heteroorganic Compounds, University of Łódź, Łódź, Poland;* [e]*LC Vision, LLC, Inc., Boulder, CO 80305, USA*

(*Received 14 December 2012; final version received 4 February 2013*)

(*E*)-4-Decenyl **2** and a series of pentenyloxy **3** derived from 2,3-difluoro-4-(2-(*trans*-4-pentylcyclohexyl) ethyl)biphenyl and an analogues series of pentenyloxy derivatives of 2,2′,3-trifluoro-4-(2-(*trans*-4-pentylcyclohexyl)ethyl)biphenyl (**4**), in which the position and configuration of the C=C bond was varied, were investigated. All materials exhibit a nematic phase, while compounds **2** and **4** also display a SmA phase. The dependence of T_{NI} on the position and configuration of the C=C bond follows the order 2-(*E*) > 4 > none > 3-(*Z*) > 3-(*E*) for series **3** and is similar for series **4**. Dielectric parameters, elastic constants and rotational viscosity were obtained as function of temperature and compared to those of their saturated analogues: decyl **1** and pentyloxy **3a** and **4a**. Dielectric anisotropy is lower for difluorobiphenyl mesogens **3** ($\Delta\varepsilon = -1.4$ to -1.8 at $\Delta T =$ –40 K) than for **4b** ($\Delta\varepsilon =$ –2.8 at $\Delta T =$ –40 K). The unsaturation in series **3** generally lowers the elastic constants K_{11} and K_{33} and their temperature dependence, and also increases rotational viscosity activation energy E_a, which follows the order: none < 3-(*Z*) < 4 < 2-(*E*) < 3-(*E*).

Keywords: nematics; negative $\Delta\varepsilon$; synthesis; electo-optics; structure-property relationship

1. Introduction

Liquid crystals containing laterally fluorinated biphenyls [1–10] are useful for applications in the flat panel display technology.[11–13] Recently, we reported difluorobiphenyl derivative **1** and investigated the effect of oxygen- and fluorine-containing substituents (–COO–, $–CH_2O–$, $–R_f$) in the decyl chain ($R=C_{10}H_{21}$) on thermal and electro-optical properties.[14] We demonstrated that modification of the chain allows control of the balance between nematic and smectic phases with only small impact on rotational viscosity γ_1 and splay elastic constant K_{11}.[14] Placement of a carbon–carbon double bond in the terminal chain provides yet another means of control of thermal and electro-optical properties of liquid crystals.[15–17] Earlier studies showed that these parameters of a mesogen depend on the position and configuration of the double bond in the peripheral chain.[18] Therefore, we investigated the unsaturated analogue of **1**, the *trans*-decenyl derivative **2** and expanded our studies to investigate the effect of the introduction of a C–C double bond in the pentyloxy chain of **3a** on mesogenic and electro-optical properties in unsaturated analogues **3b-3d**. Series **3** mesogens were compared to the analogous series of trifluorobiphenyls **4**.

In this report, we describe the synthesis of olefin **2** along with series **3** and **4** in which the position and the configuration of the C–C double bond are varied systematically. We report the effect of the double bond and the number of fluorine atoms on thermal properties, dielectric permittivity, elastic constants and rotational viscosity of the mesogens.

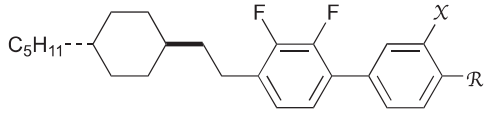

1, $\mathcal{X}$ = H: $\mathcal{R}$ = $(CH_2)_3$–*CH_2CH_2*–$(CH_2)_4CH_3$
2, $\mathcal{X}$ = H: $\mathcal{R}$ = $(CH_2)_3$–*CH=CH*–$(CH_2)_4CH_3$-(*E*)
3, $\mathcal{X}$ = H **a**: $\mathcal{R}$ = $–O(CH_2)_4CH_3$
4, $\mathcal{X}$ = F **b**: $\mathcal{R}$ = $–O(CH_2)_3CH=CH_2$
c-E: $\mathcal{R}$ = $–O(CH_2)_2CH=CHCH_3$-(*E*)
c-Z: $\mathcal{R}$ = $–O(CH_2)_2CH=CHCH_3$-(*Z*)
d-E: $\mathcal{R}$ = $–OCH_2CH=CHCH_2CH_3$-(*E*)

*Corresponding author. Email: piotr.kaszynski@vanderbilt.edu

2. Results and discussion

2.1 Synthesis

Compounds in series **3** and **4** were prepared from phenols **5** and **6**, respectively, and appropriate halide or tosylate **7** (Scheme 1). An attractive alternative to the alkylation method, is the Mitsunobu reaction. Thus, compound **4d-E** was obtained directly from phenol **6** and *trans*-2-penten-1-ol in the presence of di-isopropyl azodicarboxylate (DIAD) and PPh_3 in 77% yield.

The required phenols **5** and **6** were obtained by treatment of the corresponding methyl ethers **8** and **9** with BBr_3. The ethers **8** and **9** were prepared by Pd-catalyzed coupling of boronic acid **10** with appropriate haloanisole (Scheme 2). Details of the preparation of acid **10** were described recently.[14]

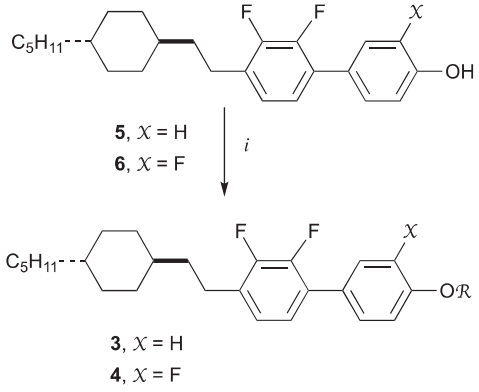

Scheme 1. Synthesis of mesogens **3** and **4**.

Note: *i*: R-Br or R-OTs, K_2CO_3, acetone, Aliquat; for **4d-E**: R-OH, DIAD, PPh_3.

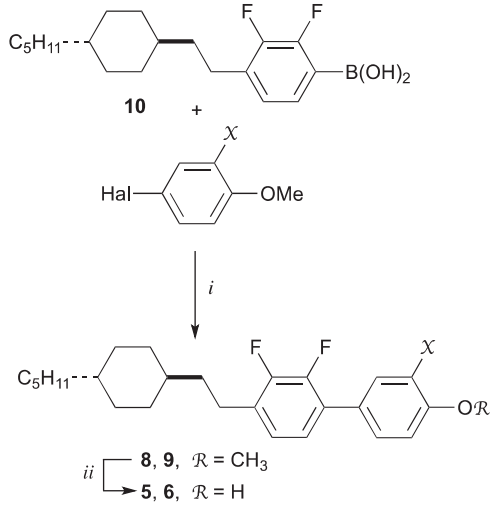

Scheme 2. Synthesis of phenols **5** and **6**.

Notes: *i*: $(PPh_3)_2PdCl_2$, 2M Na_2CO_3, benzene, EtOH, reflux, ~50%. *ii*: BBr_3, CH_2Cl_2, 99%.

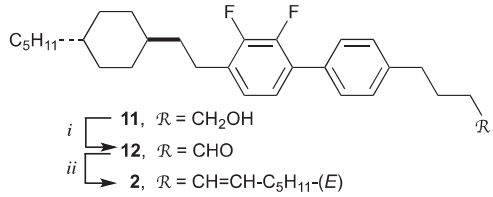

i: PCC, CH_2Cl_2, 89%. *ii*: 1. $[C_6H_{13}Ph_3P]^+Br^-$, 2. PhLi, 3. HCl in Et_2O, 4. *t*-BuOK, 40%.

Scheme 3. Synthesis of mesogen **2**.

Notes: *i*: PCC, CH_2Cl_2, 89%. *ii*: 1. $[C_6H_{13}Ph_3P]^+Br^-$, 2. PhLi, 3. HCl in Et_2O, 4. *t*-BuOK, 40%.

The tosylates **7b**,[19] **7c-E** [20,21] and **7c-Z** [21,22] were obtained from the corresponding commercial alcohols according to a literature procedure for **7c-E**.[20] The commercial *trans*-3-penten-1-ol, precursor to tosylate **7c-E** and *trans*-2-pentenyl bromide were about 90% isomerically pure. Consequently, the corresponding crude alkylation products **3** and **4** contained about 10% of the *Z* isomer, and were purified by repeated crystallisation. Compound **3c-E** was isolated isomerically pure, while **4c-E** still contained about 5% of the *Z* isomer, according to ^1H nuclear magnetic resonance (^1H NMR) spectroscopy.

Olefin **2** was prepared in 40% yield from alcohol **11**,[14] which was oxidised to aldehyde **12** and then reacted with phosphorane $Ph_3P{=}CHC_5H_{11}$ under the Wittig–Schlosser [23] conditions (Scheme 3). The isomeric purity, better than 98% of the isolated *E*-olefin, was demonstrated with 2D COSY NMR spectroscopy by the absence of through-space interactions between the two allylic CH_2 groups (C(3) and C(6), at 2.00 ppm and 2.08 ppm) of the decenyl chain.

Other approaches to olefin **2** were unsuccessful. For instance, coupling of bromide **13** with boronic acid **10** in the presence of a Pd catalyst in *N*-methyl-2-pyrrolidone (NMP) solvent resulted in isomerisation of the decenyl chain, as evident from gass chromatography-mass spectrometry (GC/MS) analysis. The aryl bromide **13** was prepared by Cu-catalyzed alkylation of 4-bromophenylmagnesium bromide with (*E*)-4-decenyl-*p*-toluenesulfonate, according to a general procedure.[24] Attempts to prepare Grignard reagents from bromides **14** or **15** for Kumada cross-coupling [25] reactions according to a general procedure [26] were also unsuccessful.

2.2 Liquid crystalline properties

Phase transition temperatures and enthalpies for olefin **2**, series **3** and **4** and also intermediates **5**, **6**, **8** and

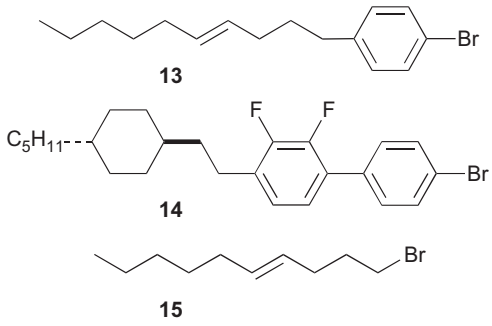

9 are presented in Table 1. For comparison purposes transition temperatures for the decyl derivative **1**, the saturated analogue of **2** is included. Phase types were assigned by comparison of microscopic textures observed in polarised light with those published for reference compounds.[27–29]

All compounds in series **1**–**6**, **8** and **9** exhibit an enantiotropic nematic phase. Smectic A phase dominates in the C_{10} derivatives **1** and **2**, and the trifluorobiphenyls **4**. A monotropic SmC phase was detected in **1** and **6**. The introduction of the *trans*-double bond to the decyl derivative **1** destabilises the nematic phase by 39 K and, to a larger extent, the SmA phase (by 44 K) in **2**. This is consistent with destabilisation of the nematic phase by nearly 30 K observed in 4-(pent-4-en-1-yl)cyclohexyl derivatives relative to the pentylcyclohexyl analogues.[16] The effect of the (*E*)-CH=CH substitution into the decyl chain on the mesophase stability is also similar to that of an ether (–CH_2O–) or ester group (–COO–).[14]

A much smaller impact of the double bond on phase stability is observed for the pentenyloxy derivatives (Figure 1). With the exception of the (*E*)-3-pentenyloxy derivative **3c-E**, all compounds in series

Table 1. Transition temperatures and enthalpies for selected compounds.[a]

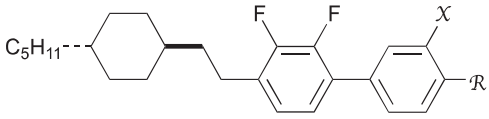

	R	X = H	X = F
1	$-(CH_2)_9CH_3$[b]	Cr ~22[c] (SmC 5)[d,e] SmA 78 N 93 I	–
2	$-(CH_2)_3CH{=}CH(CH_2)_4CH_3$-(*E*)	Cr ~5[c] SmA 34 N 54 I (0.9) (0.7)	–
		3	**4**
a	$-O(CH_2)_4CH_3$	Cr 36 N 129 I[f] (29.2) (1.7)	Cr 32 SmA 97 N 115 I (19.2) (1.0) (1.4)
b	$-O(CH_2)_3CH{=}CH_2$	Cr 30 N 134 I (36.0) (2.0)	Cr < 25 SmA 87 N 113 I (0.8) (2.0)
c-E	$-O(CH_2)_2CH{=}CHCH_3$-(*E*)	Cr 29 N 103 I (25.1) (0.8)	Cr 31 SmA 75 N 88 I (34.4) (1.2) (0.8)
c-Z	$-O(CH_2)_2CH{=}CHCH_3$-(*Z*)	Cr 39 N 120 I (30.8) (1.5)	Cr ~20 SmA 84 N 102 I (1.0) (1.5)
d-E	$-OCH_2CH{=}CHCH_2CH_3$-(*E*)	Cr 50 N 137 I (24.5) (2.1)	Cr 36 SmA 90 N 114 I (29.7) (0.6) (1.8)
		5	**6**
	–OH	Cr 155 (N 146)[d] I (38.7) (4.9)	Cr 85 (SmC 79)[d] N 118 I (24.2) (0.5) (2.9)
		8	**9**
	$-OCH_3$	Cr 55 N 139 I (37.7) (1.9)	Cr_1 71 Cr_2 73 N 121 I (28.4) (1.5)

Notes: [a]Transition temperatures (°C) and enthalpies (in italics, kJ mol^{-1}) were determined by DSC (5 K min^{-1}) in the heating mode: Cr = crystal; Sm = smectic; *I* = isotropic. [b]Data taken from ref. [14]. [c]Estimated temperature. [d]Monotropic transition. [e]Microscope observation. [f]Ref [30] Cr 27 N 107 I.

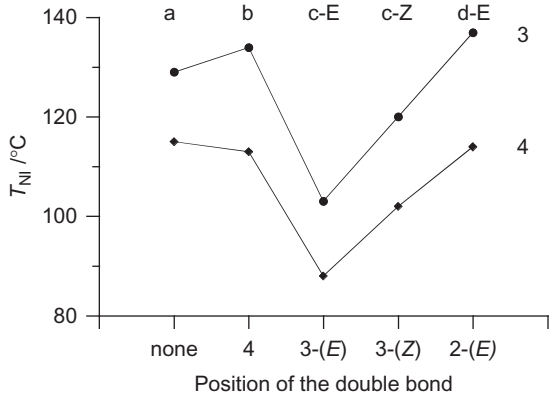

Figure 1. Clearing temperature T_{NI} for series **3** and **4** as a function of the tail structure. The lines are guide for the eye.

3 have clearing temperatures within 9 K of the pentyloxy derivative **3a**, while for **3c-E** the nematic phase is depressed by 26 K. In series **4** the trend in T_{NI} is similar to that in series **3** (Figure 1). The introduction of the third fluorine atom to **3** depresses the T_{NI} by 18 ± 4 K. Overall, the effectiveness of the double bond on nematic phase stabilisation in both series is the highest in positions 4 and 2-(*E*) of the pentenyl chain and comparable to that for the saturated analogue. This appears to be in general agreement with findings for hexenyloxycyanobiphenyls [31] and a general model developed by Kelly,[18] which shows that a *trans* C–C double bond in even positions or *cis* C–C double bond in odd position of the alkenyloxy group is favourable for high clearing temperature of the mesogen.

A pentenyloxy substituent is the shortest alkenyloxy chain used for systematic studies of the effect of the C–C double bond on mesogenic properties. Previous studies involved the hexenyloxy [31,32] and octenyloxy [33] terminal chains investigated in the cyanobiphenyl, tolanes and phenylpyrimidine derivatives, respectively. The effect of the position and configuration of the double bond on the N-I transition temperature was different in each series, and also depended on the length of the second terminal chain in the phenylpyrimidines. These studies, however, did not involve a (*E*)-3-alkenyloxy substituent. According to the general model developed by Kelly,[18] the clearing temperature for a (*E*)-3-alkenyloxy is expected to be lower than that of (*Z*)-3-alkenyloxy and this is observed experimentally for series **3** and **4** in this work. The model also predicts lower T_{NI} for the *cis* isomers of **3d-E** and **4d-E** that have not been prepared.

The pentyloxy and methoxy derivatives **3a** and **8** complement the three known members **16**–**18** of this homologous series.[1] The clearing points decrease from 139°C for the methoxy derivative **8** to 119°C for the dodecyloxy **18**, and while **3a** and **8** exhibit only a nematic phase the octyloxy derivative **16** has SmA and SmC phases.[1] Our findings significantly disagree with transition temperatures reported for **3a** in the patent literature.[30]

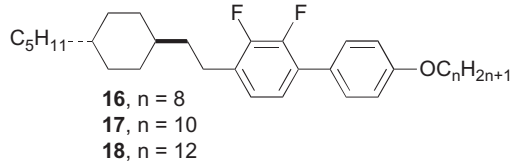

2.3 Molecular modelling

For a better understanding of the effect of the double bond and the third fluorine atom on mesogenic properties, molecular geometries of **3a** and **4a** and also model compounds **19**–**21** were optimised with the B3LYP/6-31G(d,p) method.[34]

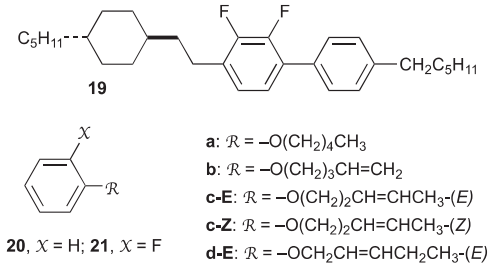

Geometry optimisation of **3a** (Figure 2) and **4a** showed little difference between the two molecules. In the most extended conformation, the penyloxy chain is coplanar with the benzene ring, the dihedral angle between the benzene ring of the biphenyl is 38° in **3a** and 37° in **4a**, the interplanar angle for the terminal alkyl chains is 45° (**3a**) and 37° (**4b**) and the total length for both molecules is 29.0 Å. The methylene analogue of **3a**, compound **19**, has similar molecular parameters with the difference being that the hexyl chain is orthogonal to the benzene ring, the interchain angle is 51° and the total molecular length is 28 Å.

Analysis of the molecular fragments **20** (Figure 2) and **21** showed that the alkenyl groups are non-planar. The interplanar angle, measured between C_{Ph}–O–CH_2 and CH_2–CH=CH, is about 60° in **b** and 66° in **c**. In (*E*)-pent-2-enyloxy derivative **20d-E** the interplanar angle is 60°, while in the fluoro analogue **21d-E** this angle is 57°. Thus, the least non-planar molecules in series **20** and **21** appear to be **20c-Z** and **21c-Z**.

2.4 Dielectric measurements

Electro-optical properties of selected compounds were measured using the single cell method [35] for series

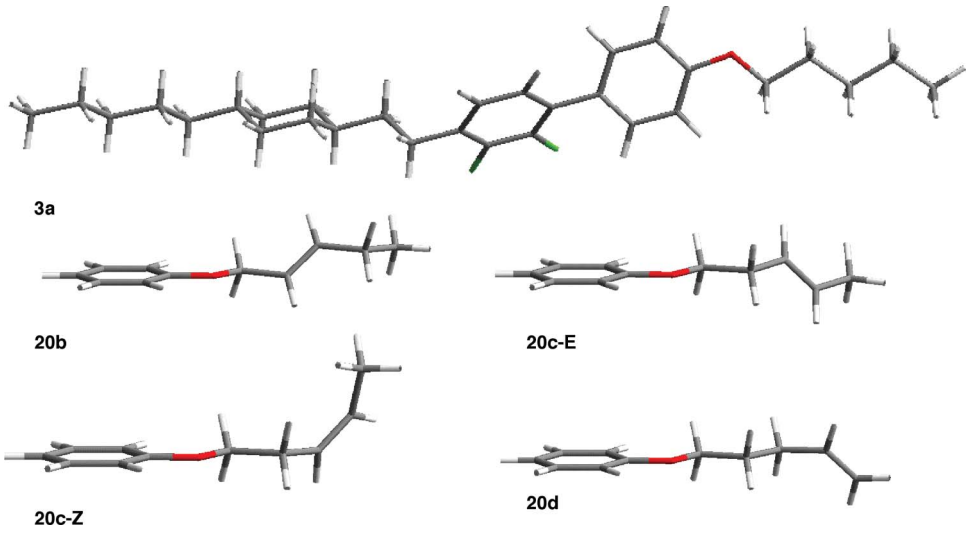

Figure 2. B3LYP/6-31G(d,p) optimised geometry of **3a** and relevant alkenyloxyphenyl fragments **20**.

3 in a broad temperature range and only for trifluorobiphenyl derivative **4b**, which exhibits the broadest nematic range in the series (26 K). For the purpose of direct comparison between compounds, dielectric and elastic constants in Table 2 are reported at the same shifted temperature $\Delta T = T - T_{NI}$. For compounds **1** and **2** ΔT was set at −10 K, due to a short range of the nematic phase in the former and nonlinear behaviour of the parameters as a function of temperature. Parameters for series **3** and **4** are reported for temperatures further away from the isotropic transition at $\Delta T = -40$ K, and typically they were obtained by interpolation of linear dependence on temperature (typical correlation factor $r^2 > 0.99$, Figures 3 and 4). Only for **4b** were values extrapolated from high temperature data collected in a range of 16 K. Rotational viscosity is reported in Table 2 at the same absolute temperature, arbitrarily chosen at 75°C.

Results show that all compounds in Table 2 are weakly polar with a small negative dielectric anisotropy. In series **3** modification of the alkyl chain in **3a** has little effect on dielectric parameters, and $\Delta\varepsilon$ is in a range of –1.4 (**3c-Z**) to –1.8 (**3b** and **3c-E**) at $\Delta T = -40$ K. However, substitution of the third fluorine atom into the biphenyl core in **3b** moderately increases the transverse dielectric components $\varepsilon_\perp$ and dielectric anisotropy $\Delta\varepsilon$ increases by 1.0 in **4b** to –2.8. Variation of the $\Delta\varepsilon$ value in series **3** is presumably due, in part, to differences in the order parameter S, which reflect conformations of the alkenyl chain (*vide supra*).

Values of splay and bend elastic constants, K_{11} and K_{33}, measured for compounds in series **3** and

Table 2. Electro-optical data for selected compounds.[a]

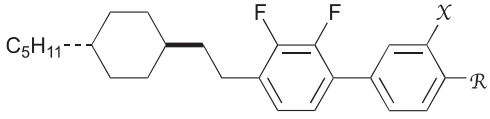

	R	T/°C	$\varepsilon_{\|\|}$	$\varepsilon_\perp$	$\Delta\varepsilon$	K_{11}/pN	K_{33}/pN	γ_1 at 75°C/mPs	E_a/kJmol^{-1}
1	$-(CH_2)_9CH_3$[b]	83[c]	3.7	3.4	−0.7	8	–	[d]	–
2	$-(CH_2)_3CH{=}CHC_5H_{11}$-*E*	44[c]	4.4	3.6	−0.8	4	–	[e]	0.86
3a	$-O(CH_2)_4CH_3$	89[f]	3.5	5.1	−1.6	42	32	166	0.45
3b	$-O(CH_2)_3CH{=}CH_2$	94[f]	3.7	5.5	−1.8	43	44	111	0.54
3c-E	$-O(CH_2)_2CH{=}CHCH_3$-*E*	63[f]	3.7	5.4	−1.8	33	24	126	0.85
3c-Z	$-O(CH_2)_2CH{=}CHCH_3$-*Z*	80[f]	3.0	4.4	−1.4	37	27	73	0.51
3d-E	$-OCH_2CH{=}CHCH_2CH_3$-*E*	97[f]	3.5	5.0	−1.5	31	31	174	0.58
4b	$-O(CH_2)_3CH{=}CH_2$	73[f,g]	3.4	6.2	−2.8	–	33	628	1.69

Notes: [a]Average of 2 sets of measurements for 2 or 3 cells. Typical standard deviation for $\varepsilon_\perp$ $\varepsilon_{||}$ and $\Delta\varepsilon < \pm 0.1$, for $K_{11} < \pm 10\%$, for $\gamma_1 < \pm 10$ mPs, and for $E_a \pm 0.01$ kJmol^{-1}. [b]Data taken from ref [14]. [c]Shifted temperature $\Delta T = T - T_{NI} = -10$ K. [d]50 mPs at 83°C. [e]220 mPs at 44°C. [f]Shifted temperature $\Delta T = T - T_{NI} = -40$ K. [g]Extrapolated from high temperature data.

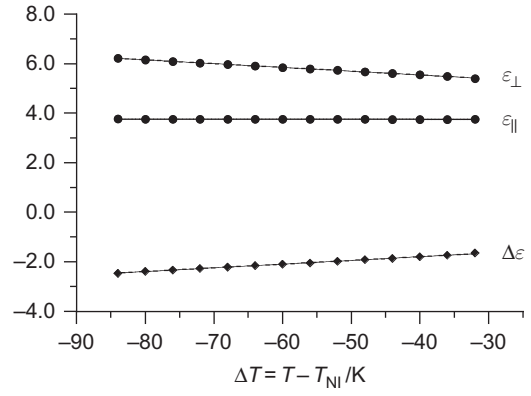

Figure 3. Dielectric permittivity as a function of temperature for **3b**. Best fit functions: $\Delta\varepsilon = 0.015 \times \Delta T - 1.20$ and $\varepsilon_\perp = -0.015 \times \Delta T + 4.93$, $r^2 = 0.999$.

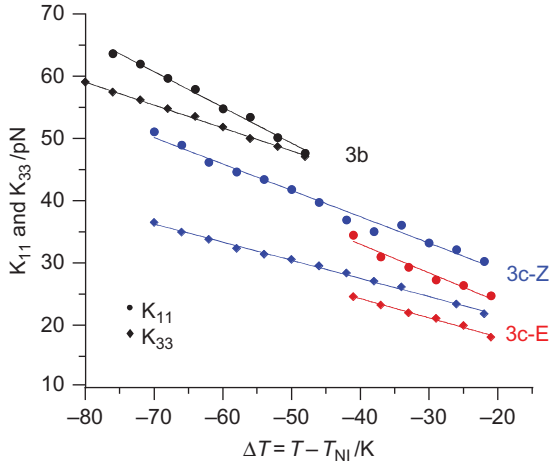

Figure 4. (colour online) Splay and bend elastic constants K_{11} (circles) and K_{33} (diamonds) for **3b** (black), **3c-Z** (blue) and **3c-E** (red) plotted as a function of shifted temperature ΔT. Best fit functions for **3b**: $K_{11} = -0.57 \times \Delta T + 20.6$ and $K_{33} = -0.37 \times \Delta T + 29.6$, $r^2 > 0.99$.

4 are typical for nematics [36] and in a range of 20–65 pN at $\Delta T < -20$ K. In general, splay elastic constants K_{11} are larger than bend elastic constants K_{33}, and they exhibit stronger dependence on temperature (Figure 4). Data in Table 2 demonstrates that incorporation of the terminal double bond into the pentyl chain of **3a** essentially does not affect the K_{11} values, while significantly increasing the K_{33} value in **3b**. Moving the double bond closer to the rigid core weakens the temperature dependence and lowers overall values of both elastic constants. The strength of the temperature dependence of K_{11} follows the order of the carbon-carbon double bond position: none > 4 > 3-(*E*) > 3-(*Z*) > 2-(*E*). It appears that incorporation of a *trans* double bond into the decyl chain of **1** lowers splay elastic constants K_{11} in **2** to about half of the value measured for **1** at $\Delta T = -10$. More in depth analysis could not be performed due to a short range of the nematic phase and non-linear behaviour of the parameters.

Substitution of the third fluorine atom into the biphenyl fragment in **4b** increases the temperature dependence of bend elastic constants K_{33}, but at $\Delta T = -40$ the extrapolated value for K_{33} is lower than that for the difluoro analogue **3b**. Unfortunately, splay elastic constants K_{11} could not be measured reliably for **4b** in this short-range nematic phase.

A comparison of rotational viscosity γ_1 at the same absolute temperature (348 K) indicates that introduction of a double bond to terminal pentyl chain in **3a** generally lowers it value (Table 2). Only in **3d-E**, in which the *trans* double bond is close to the rigid core, the value for γ_1 is slightly larger than in the saturated analogue **3a**. A particularly large effect on γ_1 is observed for the *cis* isomer **3c-Z** for which the viscosity is less than a half of that for saturated analogue **3a** at 75°C. In contrast, substitution of the third fluorine atom onto the biphenyl core markedly increases viscosity, and the γ_1 for **4b** is nearly six times larger than that for the difluoro analogue **3b** at 75°C.

Analysis of activation energy for rotational viscosity E_a in series **3** (Figure 5) indicates that modification of the pentyl chain in **3a** moderately increases the value of E_a with the largest effect, of nearly double the value, for **3c-E**. Overall the E_a values follow the order of the position of the C–C double bond: none < 3-(*Z*) <4 < 2-(*E*) < 3-(*E*). For the trifluoro derivative **4b**, E_a is greater by over three times relative to the difluoro analogue **3b**.

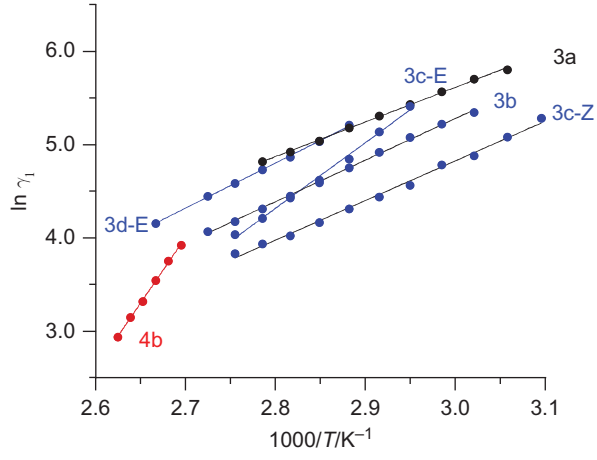

Figure 5. (colour online) Arrhenius plot of rotational viscosity γ_1 for series **3** and **4b**. Best fit function for **3b**: $\ln \gamma_1 = 4459 \times 1/T - 8.10$ and for **4b**: $\ln \gamma_1 = 14053 \times 1/T - 33.94$; $r^2 = 0.999$.

3. Summary and conclusions

Investigation of series **3** and **4** demonstrated that tuning of thermal and electro-optical properties is possible by judicious placement of the C–C double bond in the terminal alkyl chain. Analysis of the thermal data indicates that the T_{NI} is weakly affected by placing a C–C double bond in the terminal or 2-(*E*) positions, while a C–C double bond in the position 3 lowers the transition temperatures. Analysis of dielectric data for series **3** demonstrated that introduction of the double bond to the pentyl chain generally lowers rotational viscosity γ_1, moderately increases rotational viscosity activation energy E_a and lowers dependence of K_{11} on temperature.

Substituting a third lateral fluorine atom in **3** lowers the T_{NI} by an average of 18 K, induces SmA behaviour, moderately increases negative $\Delta\varepsilon$ and markedly increases rotational viscosity γ_1 and its activation energy E_a.

4. Experimental

4.1 General methods

All ^{1}H NMR spectra were obtained at 300 MHz (^{1}H) in $CDCl_3$ and referenced to tetramethylsilane (TMS). Mass spectrometry was acquired in EI mode. Optical microscopy and phase identification was performed using a Polskie Zakłady Optyczne (PZO) 'Biolar' polarised microscope equipped with a HCS250 Instec hot stage. Thermal analysis was obtained using a thermal analysis (TA) Instruments 2920 DSC (TA Instruments, New Castle, DE, USA). Transition temperatures (onset) and enthalpies were obtained using small samples (1–2 mg) and a heating rate of 5 K min-1 under a flow of nitrogen gas. For DSC and microscopic analyses, each compound was additionally purified by filtering solutions in CH_2Cl_2 to remove particles, followed by recrystallisation from appropriate solvent until constant transition temperatures. The resulting crystals were dried in vacuum overnight at ambient temperature.

4.2 Dielectric measurements and data analysis

Properties of liquid crystals were measured by Liquid Crystal Analytical System using GLCAS software version 0.951 (LCAS - Series II, LC Vision, LLC, Inc., Boulder, CO, USA).

The compounds were loaded into a pipette and filled into ITO electro-optical test cells by capillary action in the isotropic state. The cells (about 5 μm thick with an electrode area of 0.258 cm^2 and covered with a surfactant to impose a homeotropic alignment) were obtained from LC Vision LLC, and their precise thickness was measured by optical methods. The filled cells were conditioned for 12 h at a temperature that ensured the material would maintain nematic character. The liquid crystal molecules were aligned in the cell by running 5 measurements at the highest temperature before data were collected.

Default parameters were used for measuring dielectric constants of the compounds: triangular shaped voltage bias ranging from 20–0.5 V at 1 kHz frequency. The threshold voltage Vth was measured at 5% of the change. The test frequency for measuring rotational viscosity was 100 Hz or 1 kHz depending on the reliability and reproducibility of the measurements conducted at each frequency. The test voltage was set at 15 V and the repetition delay at 100 ms. Each compound was measured in 2 or 3 cells, in each cell a series of 10 measurement was repeated twice, and the datapoints averaged. Measurements were conducted typically from 50°C to 108°C depending on the material, and measurements were taken every 4 K except for compound **4b**, where measurements were taken every 2 K. The temperature was allowed to equilibrate for 5 min before measuring.

4.3 Synthesis

*4.3.1 4-((E)-Dec-4-enyl)-2′,3′-difluoro-4′-(2-(trans-4-pentylcyclohexyl)ethyl)biphenyl **(2)***

The preparation of **2** followed a general literature procedure.[23] Thus, a 1.8 M solution of PhLi in Bu_2O (1.2 mL, 2.17 mmol) was slowly added to a suspension of dry hexyl(triphenyl)phosphonium bromide (0.930 g, 2.17 mmol) in a mixture of THF (5 mL) and Et_2O (3 mL). The resulting dark red solution was cooled to –78°C, and aldehyde **12** (0.87 g, 2.0 mmol) dissolved in Et_2O (2 mL) was added. The orange solution was kept at –78°C for 5 min and then at –40°C for 10 min. An additional portion of PhLi (1.1 mL, 2.0 mmol) was added, and the resulting dark red solution was stirred and allowed to warm to –30°C. A 2.0 M solution of HCl in Et_2O (1.1 mL, 2.18 mmol) and potassium *tert*-butoxide (1.0 M solution in THF, 2.97 mL, 2.97 mmol) were added to give an orange suspension. The reaction mixture was allowed to stir for 5 h at room temperature after which the precipitate was filtered through a thin layer of silica gel (hexane). The filtrate was washed with H_2O until neutral pH was obtained. The organic layer was dried ($MgSO_4$) and the solvents were evaporated to yield 1.13 g of a yellowish liquid. The crude product was passed through a silica gel plug (hexane) and volatile impurities were removed under vacuum (100°C/0.1 mmHg). The glassy solid residue (0.83 g) was recrystallised three times (EtOH/AcOEt) at –15°C to give 0.40 g (40% yield) of olefin **2** as white needles melting at ambient temperature: ^{1}H NMR δ

0.89 (t, J = 7.2 Hz, 3H), 0.90 (t, J = 7.2 Hz, 3H), 0.80–1.05 (m, 3H), 1.15–1.21 (m, 2H), 1.25–1.40 (m, 13H), 1.51–1.57 (m, 2H), 1.70–1.86 (m, 6H), 1.97–2.03 (m, 2H), 2.05–2.10 (m, 2H), 2.66 (t, J = 7.5 Hz, 2H), 2.70 (t, J = 8.0, 2H), 5.41–5.51 (m, 2H), 6.97 (t, J = 7.1, 1H), 7.08 (td, J_1 = 7.5 Hz, J_2 = 1.2 Hz, 1H), 7.25 (d, J = 6.9 Hz, 2H), 7.45 (d, J = 7.0 Hz, 2H). Anal. Calcd for $C_{35}H_{50}F_2$: C, 82.63; H, 9.91. Found: C, 82.37; H, 9.89.

*4.3.2 Preparation of Ethers **3** and **4**. General procedure*

A mixture of phenol **5** or **6** (1 mmol), anhydrous K_2CO_3 (420 g, 3 mmol), Aliquat (cat), appropriate tosylate or alkyl bromide **7** (1.1 mmol) and acetone (50 mL) was refluxed for 24 h. Acetone was evaporated, the residue was dissolved in hexanes and passed through a silica gel plug (hexane/CH_2Cl_2, 6:1). The resulting crude ether **3** or **4** was obtained in a typical yield of better than 85% and was purified further by repeated recrystallisation from *iso*-octane, MeCN or MeOH containing EtOAc.

*4.3.3 2,3-Difluoro-4-(2-(trans-4-pentylcyclohexyl) ethyl)-4′-pentyloxybiphenyl **(3a)***

^{1}H NMR δ 0.88 (t, J = 7.1 Hz, 3H), 0.94 (t, J = 7.1 Hz, 3H), 0.92–1.03 (m, 4H), 1.11–1.33 (m, 10H), 1.34–1.52 (m, 6H), 1.69–1.88 (m, 6H), 2.68 (br t, J = 7.9 Hz, 2H), 4.00 (t, J = 6.5 Hz, 2H), 6.96 (d, J = 8.5 Hz, 2H), 6.91–6.99 (m, 1H), 7.06 (t, J = 7.6 Hz, 1H), 7.45 (d, J = 8.4 Hz, 2H). Anal. Calcd for $C_{30}H_{42}F_2O$: C, 78.91; H, 9.27. Found: C, 78.67; H, 9.46.

*4.3.4 2,3-Difluoro-4-(2-(trans-4-pentylcyclohexyl) ethyl)-4′-(pent-4-enyloxy)biphenyl **(3b)***

^{1}H NMR δ 0.88 (t, J = 7.2 Hz, 3H), 0.92–1.03 (m, 4H), 1.13–1.35 (m, 10H), 1.46–1.58 (m, 2H), 1.69–1.85 (m, 4H), 1.91 (quint, J = 6.9 Hz, 2H), 2.26 (q, J = 7.2 Hz, 2H), 2.68 (br t, J = 8.1 Hz, 2H), 4.01 (t, J = 6.4 Hz, 2H), 5.01 (dd, J_1 = 10.1 Hz, J_2 = 0.8 Hz, 1H), 5.04 (dd, J_1 = 17.2 Hz, J_2 = 1.7 Hz, 1H), 5.87 (ddt, J_1 = 17.0 Hz, J_2 = 10.0 Hz, J_3 = 6.7 Hz, 1H), 6.96 (d, J = 8.7 Hz, 2H), 6.90–7.00 (m, 1H), 7.06 (td, J_1 = 8.2 Hz, J_2 = 1.4 Hz, 1H), 7.45 (dd, J_1 = 8.7 Hz, J_2 = 1.4 Hz, 2H). Anal. Calcd for $C_{30}H_{40}F_2O$: C, 79.26; H, 8.87. Found: C, 79.09; H, 8.80.

*4.3.5 (E)-2,3-Difluoro-4-(2-(trans-4-pentyl-cyclohexyl)ethyl)-4′-(pent-3-enyloxy)biphenyl **(3c-E)***

^{1}H NMR δ 0.88 (t, J = 6.8 Hz, 3H), 0.90–1.01 (m, 4H), 1.13–1.35 (m, 10H), 1.48–1.59 (m, 2H), 1.65–1.69 (m, 3H), 1.61–1.87 (m, 4H), 2.49 (q, J = 7.2 Hz, 2H), 2.68 (br t, J = 7.9 Hz, 2H), 4.01 (t, J = 6.9 Hz, 2H), 5.49–5.65 (m, 2H), 6.96 (d, J = 8.8 Hz, 2H), 6.90–6.99 (m, 1H), 7.06 (td, J_1 = 8.4 Hz, J_2 = 1.6 Hz, 1H), 7.45 (dd, J_1 = 8.8 Hz, J_2 = 1.5 Hz, 2H). Anal. Calcd for $C_{30}H_{40}F_2O$: C, 79.26; H, 8.87. Found: C, 79.26; H, 8.93.

*4.3.6 (Z)-2,3-Difluoro-4-(2-(trans-4-pentyl-cyclohexyl)ethyl)-4′-(pent-3-enyloxy)biphenyl **(3c-Z)***

^{1}H NMR δ 0.88 (t, J = 6.8 Hz, 3H), 0.81–1.02 (m, 4H), 1.12–1.34 (m, 10H), 1.48–1.54 (m, 2H), 1.65–1.69 (m, 3H), 1.70–1.86 (m, 4H), 2.57 (q, J = 7.0 Hz, 2H), 2.69 (br t, J = 8.0 Hz, 2H), 4.01 (t, J = 7.0 Hz, 2H), 5.44–5.56 (m, 1H), 5.57–5.69 (m, 1H), 6.97 (d, J = 8.7 Hz, 2H), 6.91–7.00 (m, 1H), 7.06 (td, J_1 = 8.3 Hz, J_2 = 1.4 Hz, 1H), 7.45 (dd, J_1 = 8.4 Hz, J_2 = 1.5 Hz, 2H). Anal. Calcd for $C_{30}H_{40}F_2O$: C, 79.26; H, 8.87. Found: C, 79.04; H, 8.87.

*4.3.7 (E)-2,3-Difluoro-4-(2-(trans-4-pentyl-cyclohexyl)ethyl)-4′-(pent-2-enyloxy)biphenyl **(3d-E)***

^{1}H NMR δ 0.88 (t, J = 6.6 Hz, 3H), 0.82–0.99 (m, 4H), 1.04 (t, J = 7.4 Hz, 4H) 1.11–1.34 (m, 10H), 1.47–1.54 (m, 2H), 1.69–1.88 (m, 4H), 2.13 (quint, J = 6.8 Hz, 2H), 2.68 (br t, J = 7.9 Hz, 2H), 4.51 (dd, J_1 = 6.0 Hz, J_2 = 0.9 Hz, 2H), 5.65–5.78 (m, 1H), 5.86–5.97 (m, 1H), 6.97 (d, J = 8.7 Hz, 2H), 6.91–7.01 (m, 1H), 6.98 (d, J = 8.8 Hz, 1H), 6.98 (td, J_1 = 8.2 Hz, J_2 = 1.4 Hz, 1H), 7.45 (dd, J_1 = 8.6 Hz, J_2 = 1.3 Hz, 2H). Anal. Calcd for $C_{30}H_{40}F_2O$: C, 79.26; H, 8.87. Found: C, 79.41; H, 9.04.

*4.3.8 2,3,3′-Trifluoro-4-(2-(trans-4-pentyl-cyclohexyl)ethyl)-4′-pentyloxybiphenyl **(4a)***

^{1}H NMR δ 0.88 (t, J = 7.2 Hz, 3H), 0.94 (t, J = 7.2 Hz, 3H), 0.92–1.03 (m, 4H), 1.15–1.35 (m, 10H) 1.38–1.55 (m, 6H), 1.69–1.90 (m, 6H), 2.68 (br t, J = 8.0 Hz, 2H), 4.07 (t, J = 6.5 Hz, 2H), 6.92–7.07 (m, 3H), 7.20–7.32 (m, 2H). Anal. Calcd for $C_{30}H_{41}F_3O$: C, 75.91; H, 8.71. Found: C, 75.75; H, 8.73.

*4.3.9 2,3,3′-Trifluoro-4-(2-(trans-4-pentyl-cyclohexyl)ethyl)-4′-(pent-4-enyloxy)biphenyl **(4b)***

^{1}H NMR δ 0.88 (t, J = 6.9 Hz, 3H), 0.82–1.01 (m, 4H), 1.13–1.34 (m, 10H), 1.47–1.55 (m, 2H), 1.72–1.83 (m, 4H), 1.95 (quint, J = 6.9 Hz, 2H), 2.27 (q, J = 7.1 Hz, 2H), 2.68 (bt, J = 8.0 Hz, 2H), 4.09 (t, J = 6.4 Hz, 2H), 5.02 (d, J = 10.2 Hz, 1H), 5.08 (dd, J_1 = 17.1 Hz, J_2 = 1.6 Hz, 1H), 5.86 (ddt, J_1 = 17.0 Hz, J_2 = 10.3 Hz, J_3 = 6.6 Hz, 1H), 6.93–7.07 (m, 3H), 7.21–7.31 (m,

2H). Anal. Calcd for $C_{30}H_{39}F_3O$: C, 76.24; H, 8.32. Found: C, 76.58; H, 8.44.

4.3.10 (E)-2,3,3′-Trifluoro-4-(2-(trans-4-pentylcyclohexyl)ethyl)-4′-(pent-3-enyloxy)biphenyl ***(4c-E)***

^{1}H NMR δ 0.88 (t, $J = 6.6$ Hz, 3H), 0.80–1.13 (m, 4H), 1.13–1.34 (m, 10H), 1.47–1.58 (m, 2H), 1.65–1.69 (m, 3H), 1.71–1.87 (m, 4H), 2.52 (q, $J = 6.5$ Hz, 2H), 2.69 (br t, $J = 7.9$ Hz, 2H), 4.07 (t, $J = 6.9$ Hz, 2H), 5.46–5.68 (m, 2H), 6.92–7.07 (m, 3H), 7.20–7.32 (m, 2H). Anal. Calcd for $C_{30}H_{39}F_3O$: C, 76.24; H, 8.32. Found: C, 76.21; H, 8.31.

4.3.11 (Z)-2,3,3′-Trifluoro-4-(2-(trans-4-pentylcyclohexyl)ethyl)-4′-(pent-3-enyloxy)biphenyl ***(4c-Z)***

^{1}H NMR δ 0.88 (t, $J = 6.8$ Hz, 3H), 0.81–1.13 (m, 4H), 1.13–1.34 (m, 10H), 1.47–1.58 (m, 2H), 1.65–1.69 (m, 3H), 1.70–1.85 (m, 4H), 2.61 (q, $J = 7.2$ Hz, 2H), 2.69 (br t, $J = 8.0$ Hz, 2H), 4.08 (t, $J = 7.0$ Hz, 2H), 5.44–5.55 (m, 1H), 5.58–5.71 (m, 1H), 6.92–7.09 (m, 3H), 7.21–7.32 (m, 2H). Anal. Calcd for $C_{30}H_{39}F_3O$: C, 76.24; H, 8.32. Found: C, 76.44; H, 8.16.

4.3.12 (E)-2,3,3′-Trifluoro-4-(2-(trans-4-pentylcyclohexyl)ethyl)-4′-(pent-2-enyloxy)biphenyl ***(4d-E)***

To a mixture of *trans*-2-penten-1-ol (16 mg, 0.18 mmol), phenol **6** (65 mg, 0.16 mmol), PPh_3 (50 mg, 0.19 mmol) in dry THF (2 mL), di-isopropyl azodicarboxylate (DIAD) was added at 0°C under Ar. The mixture was stirred at room temperature for 3 days, water was added, the organic layer was separated, dried ($NaSO_4$) and the solvent was evaporated. The resulting residue was passed through a silica gel plug (hexane/CH_2Cl_2, 5:1) to give 58 mg (77% yield) of **4d-E** as a white solid. An analytically pure sample was obtained by repeated recrystallisation from EtOH/EtOAc, MeCN and *iso*-octane (–78°C): ^{1}H NMR δ 0.88 (t, $J = 7.0$ Hz, 3H), 0.84–1.00 (m, 4H), 1.03 (t, $J = 7.5$ Hz, 3H), 1.12–1.34 (m, 10H), 1.48–1.56 (m, 2H), 1.71–1.85 (m, 4H), 2.12 (quin, $J = 6.9$ Hz, 2H), 2.69 (br t, $J = 8.0$ Hz, 2H), 4.59 (d, $J = 6.2$ Hz, 2H), 5.68–5.77 (m, 1H), 5.87–5.97 (m, 1H), 6.93–7.00 (m, 1H), 7.00–7.07 (m, 2H), 7.20–7.32 (m, 2H). Anal. Calcd for $C_{30}H_{39}F_3O$: C, 76.24; H, 8.32. Found: C, 76.52; H, 8.27.

4.3.13 2′,3′-Difluoro-4′-(2-(trans-4-pentylcyclohexyl)ethyl)biphenyl-4-ol ***(5)***

A solution of anisole **8** (4.75 g, 11.0 mmol) was treated with BBr_3 (22 mL, 22 mmol, 1.0 M solution in CH_2Cl_2) and the reaction mixture was stirred overnight at room temperature. Water (10 mL) was added slowly, the reaction mixture was stirred for 30 min, the organic layer was separated and washed with $NaHCO_3$. The organic layer was then dried (Na_2SO_4) and evaporated to afford 4.25 g (99% yield) of phenol **5** as a crystalline solid. An analytically pure sample of phenol **5** was obtained by repeated crystallisation from MeCN: ^{1}H NMR δ 0.88 (t, $J = 6.6$ Hz, 3H), 0.84–1.02 (m, 4H), 1.12–1.34 (m, 10H), 1.47–1.57 (m, 2H), 1.70–1.85 (m, 4H), 2.68 (br t, $J = 8.1$ Hz, 2H), 4.83 (s, 1H), 6.90 (d, $J = 8.8$ Hz, 2H), 6.95 (t, $J = 7.6$ Hz, 1H), 7.05 (t, $J = 7.4$ Hz, 1H), 7.42 (d, $J = 7.8$ Hz, 2H). Anal. Calcd for $C_{25}H_{32}F_2O$: C, 77.69; H, 8.34. Found C, 77.62; H, 8.42.

4.3.14 -2′3′3-Trifluoro-4′-(2-(trans-4-pentylcyclohexyl)ethyl)biphenyl-4-ol ***(6)***

Obtained from anisole **9** as described above for the preparation of **5**. An analytically pure sample of **6** was obtained by repeated recrystallisation from MeCN: ^{1}H NMR (400 MHz) δ 0.88 (t, $J = 6.8$ Hz, 3H), 0.82–1.02 (m, 4H), 1.13–1.34 (m, 10H), 1.47–1.57 (m, 2H), 1.72–1.88 (m, 4H), 2.69 (br t, $J = 7.8$ Hz, 2H), 5.18 (d, $J = 4.2$ Hz, 1H), 6.96 (t, J, $= 7.4$ Hz, 1H), 7.04 (td, $J_1 = 7.4$ Hz, $J_2 = 1.4$ Hz, 1H), 7.07 (t, $J = 8.7$ Hz, 1H), 7.21 (t, $J = 8.7$ Hz, 1H), 7.29 (d, $J = 11.7$ Hz, 1H). Anal. Calcd for $C_{25}H_{31}F_3O$: C, 74.23; H, 7.72. Found: C, 73.96; H, 7.61.

4.3.15 4-Pentenyl p-Toluenesulfonate [19] ***(7b)***

A solution of tosyl chloride (1.91 g, 10 mmol) in dry pyridine (10 mL) was treated with a pyridine solution (5 mL) of 4-penten-1-ol (750 mg, 8.72 mmol) at 0°C. The mixture was stirred at 0°C for 4 h, 10% HCl (50 mL) was added and the mixture was extracted with CH_2Cl_2. The CH_2Cl_2 extract was washed with sat. $NaHCO_3$, dried (Na_2SO_4) and the solvent was evaporated to give 1.84 g (88% yield) of tosylate **7b** as an oil: ^{1}H NMR δ 1.74 (quin, $J = 6.9$ Hz, 2H), 2.03–2.12 (m, 2H), 2.45 (s, 3H), 4.03 (t, $J = 6.4$ Hz, 2H), 4.90–5.00 (m, 2H), 5.61–5.76 (m, 1H), 7.34 (d, $J = 7.9$ Hz, 2H), 7.78 (d, $J = 8.3$ Hz, 2H).

4.3.16 2,3-Difluoro-4′-methoxy-4-(2-(trans-4-pentylcyclohexyl)ethyl)biphenyl ***(8)***

A mixture of 2,3-difluoro-4-(2-(*trans*-4-pentylcyclohexyl)ethyl)phenylboronic acid [14] (**10**, 7.0 g, 20.7 mmol), *p*-bromoanisole (4.57 g, 22.3 mmol) and K_2CO_3 (5.7 g, 41 mmol) in DMF (50 mL) under N_2 was added into fresh $(Ph_3)_4Pd$ (600 mg, 0.5 mmol). The mixture was stirred at 80°C for 48 h and filtered through Cellite. Water (100 mL) was added and the

mixture was extracted with EtOAc (3 × 50 mL). The organic layers were combined and dried (Na_2SO_4) and the solvent was evaporated. The residue was passed through a silica gel plug (hexane followed by hexane/CH_2Cl_2, 2:1) and further purified by crystallisation (*i*-octane) to give 4.39 g (53% yield) of anisole **8** as a crystalline solid. An analytical sample was obtained by recrystallisation from MeCN: ^{1}H NMR δ 0.88 (t, $J = 7.1$ Hz, 3H), 0.82–1.03 (m, 4H), 1.12–1.35 (m, 10H), 1.47–1.57 (m, 2H), 1.72–1.85 (m, 4H), 2.69 (br t, $J = 8.0$ Hz, 2H), 3.85 (s, 3H), 6.98 (d, $J = 8.9$ Hz, 2H), 6.92–7.01 (m, 1H), 7.06 (td, $J_1 = 8.4$ Hz, $J_2 = 1.6$ Hz, 1H), 7.47 (dd, $J_1 = 8.8$ Hz, $J_2 = 1.5$ Hz, 2H). Anal. Calcd for $C_{26}H_{34}F_2O$: C, 77.96; H, 8.56. Found: C, 78.08; H, 8.67.

4.3.17 2,3,3′-Trifluoro-4′-methoxy-4-(2-(trans-4-pentylcyclohexyl)ethyl)biphenyl ***(9)***

The compound **9** was obtained from boronic acid **10** [14] (6.0 g, 17.7 mmol) and 4-bromo-2-fluoroanisole (4.35 g, 21.3 mmol), as described for the preparation of **8**. The crude product was purified by recrystallisation (*iso*-octane) to give 3.44 g (46% yield) of anisole **9** as a crystalline solid: ^{1}H NMR δ 0.88 (t, $J = 7.2$ Hz, 3H), 0.82–1.03 (m, 4H), 1.08–1.33 (m, 10H), 1.46–1.55 (m, 2H), 1.72–1.86 (m, 4H), 2.68 (br t, $J = 8.0$ Hz, 2H), 3.93 (s, 3H), 6.92–7.09 (m, 3H), 7.26–7.32 (m, 2H). Anal. Calcd for $C_{26}H_{33}F_3O$: C, 74.61; H, 7.95. Found: C, 74.83; H, 8.08.

4.3.18 4-(2′,3′-Difluoro-4′-(2-(trans-4-pentylcyclohexyl)ethyl)biphenyl-4-yl)butanal ***(12)***

A mixture of PCC (0.72 g, 3.33 mmol) and alcohol **11** [14] (0.98 g, 2.22 mmol) in dry CH_2Cl_2 (15 mL) was stirred for 3 h at room temperature. The reaction progress was monitored by TLC (CH_2Cl_2/hexane, 1:1) until the starting alcohol was no longer observed. Additional portions of PCC (10 mg) were added as necessary to complete the oxidation. Dry Et_2O (10 mL) was added and the organic layer was separated from the black residue. The combined organic layers were passed through a silica gel plug (Et_2O), solvents were removed and the resulting glassy solid was dried in vacuum to give 0.87 g (89% yield) of aldehyde **12** as a white solid: ^{1}H NMR δ 0.88 (t, $J = 5.9$ Hz, 3H), 0.80–1.05 (m, 3H), 1.15–1.40 (m, 11H), 1.47–1.58 (m, 2H), 1.72–1.88 (m, 4H), 2.00 (quint, $J = 7.0$ Hz, 2H), 2.50 (t, $J = 7.2$ Hz, 2H), 2.65–2.75 (m, 4H) 6.97 (t, $J = 7.2$ Hz, 1H), 7.08 (t, $J = 7.4$, 1H), 7.24 (d, $J = 7.7$ Hz, 2H), 7.45 (d, $J = 7.8$ Hz, 2H), 9.80 (s, 1H).

The aldehyde was used in the subsequent step without further purification.

Acknowledgements

Partial financial support for this work was received from the National Science Foundation (DMR-0606317 and DMR-1207585). We thank Ms. Lillian E. Johnson for her assistance with dielectric measurements.

References

[1] Hird M, Gray GW, Toyne KJ. The synthesis and transition temperatures of some trans-4-alkylcyclohexylethyl-substituted 2,3-difluorobiphenyls. Liq Cryst. 1992;11:531–546.
[2] Hird M, Toyne KJ, Slaney AJ, Goodby JW. Synthesis and transition temperatures of host materials for ferroelectric mixtures. J Mater Chem. 1995;5:423–430.
[3] Kirsch P, Reiffenrath V, Bremer, M. Nematic liquid crystals with negative dielectric anisotropy: molecular design and synthesis. Synlett. 1999:389–396.
[4] Bremer M, Lietzau L. 1,1,6,7-Tetrafluoroindanes: improved liquid crystals for LCD-TV application. New J. Chem. 2005;29:72–74.
[5] Januszko A, Glab KL, Kaszynski P, Patel K, Lewis RA, Mehl GH, Wand MD. The effect of carborane, bicyclo[2.2.2]octane and benzene on mesogenic and dielectric properties of laterally fluorinated three-ring mesogens. J Mater Chem. 2006;16:3183–3192.
[6] Hird M. Fluorinated liquid crystals – properties and applications. Chem Soc Rev. 2007;36:2070–2095.
[7] Goodby JW, Saez IM, Cowling SJ, Gasowska JS, MacDonald RA, Sia S, Watson P, Toyne KJ, Hird M, Lewis RA, Lee S-E, Vaschenko V. Molecular complexity and the control of self-organising processes. Liq Cryst. 2009;36:567–605.
[8] Jiang Y, An Z, Chen P, Chen X, Zheng M. Synthesis and mesomorphic properties of but-3-enyl-based fluorinated biphenyl liquid crystals. Liq Cryst. 2012;39:457–465.
[9] Jiang Y, Lu L, Chen P, Chen X, Li J, An Z. Synthesis and properties of allyloxy-based biphenyl liquid crystals with multiple lateral fluoro substituents. Liq Cryst. 2012;39:957–963.
[10] Dziaduszek J, Kula P, Dąbrowski R, Drzewiński W, Garbat K, Urban S, Gauza S. General synthesis method of alkyl–alkoxy multi-fluorotolanes for negative high birefringence nematic mixtures. Liq Cryst. 2012;39:239–247.
[11] Kirsch P, Bremer, M. Nematic liquid crystals for active matrix displays: molecular design and synthesis. Angew Chem Int Ed Engl. 2000;39:4216–4235.
[12] Pauluth D, Tarumi K. Advanced liquid crystals for television. J Mater Chem. 2004;14:1219–1227.
[13] Goodby JW. The nanoscale engineering of nematic liquid crystals for displays. Liq. Cryst. 2011;38:1363–1387.
[14] Jankowiak A, Januszko A, Ringstrand B, Kaszynski P. New series of liquid crystals with negative dielectric anisotropy. Liq Cryst. 2008;35:65–77.
[15] Petrzilka M. New liquid crystals: the synthesis and mesomorphic properties of nematic alkenylsubstituted cyanophenylcyclohexanes. Mol Cryst Liq Cryst. 1985;131:109–123.
[16] Schadt M, Buchecker R, Leenhouts F, Boller A, Villiger A, Petrzilka M. New nematic liquid crystals:

influence of rigid cored, alkenyl side-chains and polarity on material and display properties. Mol Cryst Liq Cryst. 1986;139:1–25.
[17] Schadt M, Buchecker R, Müller K. Invited lecture. Material properties, structural relations with molecular ensembles and electro-optical performance of new bicyclohexane liquid crystals in field-effect liquid crystal displays. Liq Cryst. 1989;5:293–312.
[18] Kelly SM. The effect of the position and configuration of carbon–carbon double bonds on the mesomorphism of thermotropic, non-amphiphilic liquid crystals. Liq Cryst. 1996;20:493–515.
[19] White JD, Hrnciar P. Synthesis of polyhydroxylated pyrrolizidine alkaloids of the alexine family by tandem ring-closing metathesis − transannular cyclization. (+)-Australine. J Org Chem. 2000;65:9129–9142.
[20] Scheideman M, Shapland P, Vedejs E. Mechanistic alternative for the intramolecular hydroboration of homoallylic amine and phosphine borane complexes. J Am Chem Soc. 2003;125:10502–10503.
[21] Dobbs AP, Guesné SJJ, Parker RJ, Skidmore J, Stephenson RA, Hursthouse MB. A detailed investigation of the aza-Prins reaction. Org Biomol Chem. 2010;8:1064–1080.
[22] Servis KL, Roberts JD. Small-ring compounds. XLIII. Formolysis of substituted allylcarbinyl tosylates. J Am Chem Soc. 1965;87:1331–1339.
[23] Schlosser M, Christmann KF. Trans-selective olefin syntheses. Angew Chem Int Ed Engl. 1966;5:126.
[24] Cahiez G, Chaboche C, Jézéquel M. Cu-catalyzed alkylation of grignard reagents: a new efficient procedure. Tetrahedron. 2000;56:2733–2737.
[25] Tamao K, Sumitani K, Kiso Y, Zembayashi M, Fujioka A, Kodama S, Nakajima I, Minato A, Kumada M. Nickel-phosphine complex-catalyzed grignard coupling. I. Cross-coupling of alkyl, aryl, and alkenyl grignard reagents with aryl and alkenyl halides: general scope and limitations. Bull Chem Soc Jpn. 1976;49: 1958–1969.
[26] Plaut DJ, Martin SM, Kjaer K, Weygand MJ, Lahav M, Leiserowitz L, Weissbuch I, Ward MD. Structural characterization of crystalline ternary inclusion compounds at the air − water interface. J Am Chem Soc. 2003;125:15922–15934.
[27] Demus D, Richter L. Textures of liquid crystals. 2nd ed. Leipzig: VEB; 1980.
[28] Gray GW, Goodby JWG. Smectic liquid crystals-textures and structures. Philadelphia (PA): Leonard Hill; 1984.
[29] Dierking I. Textures of liquid crystals. Weinheim: Wiley-VCH; 2003.
[30] Reiffenrath V, Krause J, Waechtler A, Weber G, Finkenzeller U, Coates D, Sage IC, Greenfield S, Gray GW, Hird M, Lacey D, Toyne KJ. 2,3-Difluorobiphenyls. Ger. Offen. DE 3.807.861;1989.
[31] Duffy WL, Jones JC, Kelly SM, Minter V, Tuffin RP. Synthesis and evaluation of nematic 4-alkenyloxy- and 4-alkenoyloxy-4′-cyanobiphenyls. Mol Cryst Liq Cryst. 1999;332:101–108.
[32] Skelton GW, Dong D, Tuffin RP, Kelly SM. Nematic tolanes and acetylenes. J Mater Chem. 2003;13:450–457.
[33] Kelly SM. 2-[4-Alkenyloxy)phenyl]-5-alkylpyrimidines The relationship between position and nature (E/Z) of the double bond and transition temperatures. Liq Cryst. 1993;14:675–698.
[34] Frisch MJ, Trucks GW, Schlegel HB, Scuseria GE, Robb MA, Cheeseman JR, Scalmani G, Barone V, Mennucci B, Petersson GA, Nakatsuji H, Caricato M, Li X, Hratchian HP, Izmaylov AF, Bloino J, Zheng G, Sonnenberg JL, Hada M, Ehara M, Toyota K, Fukuda R, Hasegawa J, Ishida M, Nakajima T, Honda Y, Kitao O, Nakai H, Vreven T, Montgomery JA Jr, Peralta JE, Ogliaro F, Bearpark M, Heyd JJ, Brothers E, Kudin KN, Staroverov VN, Keith T, Kobayashi R, Normand J, Raghavachari K, Rendell A, Burant JC, Iyengar SS, Tomasi J, Cossi M, Rega N, Millam JM, Klene M, Knox JE, Cross JB, Bakken V, Adamo C, Jaramillo J, Gomperts R, Stratmann RE, Yazyev O, Austin AJ, Cammi R, Pomelli C, Ochterski JW, Martin RL, Morokuma K, Zakrzewski VG, Voth GA, Salvador P, Dannenberg JJ, Dapprich S, Daniels AD, Farkas O, Foresman JB, Ortiz JV, Cioslowski J, Fox DJ. Gaussian 09, Revision A.02. Wallingford (CT): Gaussian, Inc; 2009.
[35] Wu S-T, Coates D, Bartmann E. Physical properties of chlorinated liquid crystals. Liq. Cryst. 1991;10:635–646.
[36] Saito H. Elastic properties of nematics for applications. In: Dunmur DA, Fukuda A, Luckhurst GR, editors. Physical properties of liquid crystals: nematics. London: IEE; 2001. p. 582–591.